PHYSICAL REVIEW B **83**, 104404 (2011)

Critical behavior in the inhomogeneous ferromagnet $SrFe_{0.80}Co_{0.20}O_{3.0}$

J. Lago,[1,*] M. J. Rosseinsky,[2] S. J. Blundell,[3] P. D. Battle,[4] M. Diaz,[1] I. Uriarte,[1] and T. Rojo[1]

[1]*Departament of Inorganic Chemistry, Universidad del Païs Vasco, E-48080 Bilbao, Spain*

[2]*Department of Chemistry, University of Liverpool, Liverpool L69 7ZD, United Kingdom*

[3]*Clarendon Laboratory, Department of Physics, University of Oxford, Oxford OX1 3PU, United Kingdom*

[4]*Inorganic Chemistry Laboratory, South Parks Road, Oxford OX1 3QR, United Kingdom*

(Received 29 November 2010; published 9 March 2011)

A detailed muon spin relaxation (μSR) and magnetization study is presented of the paramagnetic-to-ferromagnetic transition in the compound $SrFe_{0.80}Co_{0.20}O_3$. The critical exponents derived from the static critical analysis are close to the theoretical predictions for the Heisenberg model in three dimensions. However, a small drift toward mean-field values is interpreted as arising from the presence of long-range dipolar interactions between the Fe(IV) centers. The evolution of spin dynamics across the transition determined from the μSR study is consistent with this interpretation. μSR and magnetization data also provide evidence of an inhomogeneous magnetic state both above and below T_c, placing this system in line with other double-exchange materials such as manganites and cobaltites where spontaneous electronic and magnetic phase separation appears conspicuous and explains much of the encountered experimental phenomenology.

DOI: 10.1103/PhysRevB.83.104404 PACS number(s): 64.60.F−, 75.40.Cx, 75.40.Gb, 76.75.+i

I. INTRODUCTION

It is now widely acknowledged that magnetoelectronic phase separation at the nanoscale is behind much of the observed phenomenology in oxide systems such as the CMR manganites, the cobaltites, or even the high-T_c cuprates.[1] In the manganites, competition between co-existing charged-ordered and ferromagnetic phases is key to understanding the low-temperature magnetoresistance found in low-bandwidth systems. First order in the clean limit, the transition between the competing phases is smeared by quenched disorder making it continuous with percolative characteristics. Phase separation occurs even in the large-bandwidth manganites in the low hole-density regime and it is responsible for the observed ferromagnetic insulating behavior in the medium/low doping regime. In the cobaltites $Ln_{1-x}Sr_xCoO_3$ magnetoelectronic separation coexists with spin state transitions that occur because of the subtle balance between the similar-sized crystal-field splitting of the 3*d* orbitals in the Co ion and the Hund's rule coupling. The result is a complex x-dependent phase diagram in which coexistence of ferromagnetic metallic (FMM) and insulating nonferromagnetic domains has been corroborated by various experimental techniques on both sides of the metal-to-insulator transition at $x_c = 0.18$. Wu and co-workers have suggested that, for x values close to x_c, the system essentially behaves as a natural analog of the artificial heterostructures displaying negative intergranular magnetoresistance (GMR).[2] This suggests that intrinsic phase inhomogenity is, as in the manganites (albeit due to a different origin), responsible for the observed physical behavior of these materials and, in particular, for their large negative magnetoresistance.

In comparison with the manganites and cobaltites, the series $SrFe_{1-x}Co_xO_{3-\delta}$ (SrFeCo) has received relatively little attention despite early indications of a complex phase diagram[3] and the report of large negative magnetoresistance for $x = 0.10$.[4] In this system an antiferromagnetic-to-ferromagnetic transition has been reported as a function of x, with inhomogeneous behavior suggested for $0.0 < x < 0.20$.[5] $SrFeO_{3.0}$ ($x = 0$) is a metallic antiferromagnet ($T_N = 134$ K) with a helicoidal spin structure with propagation vector along $\langle 111 \rangle$.[6] The metallicity in this system is a direct consequence of its particular electronic ground state, with a negative charge-transfer character (i.e., $\Delta < 0$, where Δ is the p-d band gap;[7] the ground state is in fact dominated by a $d^5\underline{L}$ configuration, where $\underline{L}$ is an oxygen hole[8]). As a result, a strong Fe 3*d*–O 2*p* hybridization occurs that gives rise to an extended σ^* band of e_g parentage in which charge carriers are holes in mainly oxygen levels. It is commonly accepted that the helical magnetic structure arises from the competition between antiferromagnetic exchange coupling between localized t_{2g} spins and ferromagnetic double-exchange interactions induced by the delocalized oxygen holes.[9] Recent calculations, however, have challenged this view and shown that double exchange alone may be sufficient to generate it.[10] At the other end of the series, $SrCoO_{3.0}$ is also a charge-transfer material with a negative gap.[11] This leads to a Co^{IV} (d^5) intermediate electronic state that is dominated by a $d^6\underline{L}$ ($t_{2g}^4 e_g^2 \underline{L}$ configuration. The system is metallic and ferromagnetic ($T_c = 280$ K).[5,11]

Co substitution in $SrFeO_{3.0}$ appears to enhance the delocalization of the e_g electrons of Fe parentage in a broadened σ^* band.[5] However, how this increased itineracy causes the observed strengthening of ferromagnetic interactions along the series is not yet completely understood. As indicated by Abbate and co-workers,[12] double exchange—-although behind the magnetic behavior of the $x = 0$[10,13] and possibly the $x = 1.0$ compositions[11]—may not provide the right mechanism for ferromagnetism in this family due to the large difference in the potential felt by the e_g electrons at the Fe and Co sites. Instead, these authors propose a picture of half metallic ferromagnetism in which Co doping induces a gap at the Fermi level in the majority e_g band thus turning the system ferromagnetic. In any case, previous experimental studies of the magnetism of $SrFe_{1-x}Co_xO_{3-\delta}$ outline a phase diagram divided into two well-defined regions: a Fe-rich one for $x \leqslant 0.20$ and a second, Co-rich region for $x > 0.20$.[5,14] The limiting composition,

$x = 0.20$, is taken to mark the onset of long-range (LRO) ferromagnetism in the series.

Competing ferro- and antiferromagnetic interactions are claimed to generate inhomogeneous magnetic behavior in the Fe-rich region.[5,14] Yet, despite the potential interest this competition might have in light of the findings in manganites and cobaltites, no serious attempt has been made to fully characterize this part of the phase diagram. We have thus embarked on a project whose aim is to map the different magnetic phases present in the low-x part of the $SrFe_{1-x}Co_xO_{3.0}$ series by means of magnetization and muon spin relaxation (μSR) studies of the phase transitions that occur at different compositions. Here we present results on the composition $SrFe_{0.80}Co_{0.20}O_{3.0}$ that show that despite the onset of LRO ferromagnetism at $T_c = 241$ K, the system remains magnetically inhomogeneous even in the ordered state.

II. EXPERIMENTAL DETAILS AND METHODS

Polycrystalline samples of $SrFe_{0.8}Co_{0.2}O_{3-\delta}$ ($\delta \simeq 0.15$) were synthesized by the standard ceramic method. Stoichiometric amounts of $SrCO_3$, Fe_2O_3, and $Co(NO_3)_2{\cdot}6H_2O$ were first preheated at 700°C and then fired at 1200°C in air for approximately 40 h. The resulting black powder was then repelletized and annealed under oxygen pressure ($P_{O_2} \sim$ 600–700 atm) at 300–350°C, which resulted in the fully stoichiometric material $SrFe_{0.8}Co_{0.2}O_{3.0}$. The quality and phase purity of the samples was determined by high-resolution neutron diffraction using the HRPD diffractometer at ISIS (RAL, UK). Ac susceptibility was measured on a Lakeshore susceptometer while dc measurements were performed with a Quantum Design superconducting quantum interference device magnetometer. The internal field h_i used for the analysis of the critical behavior was corrected for demagnetization; i.e., $h_i = H_{\text{appl}} - DM$, where D is the demagnetization factor, calculated from M vs H measurements in the low-field limit in the ordered state.

Finally, zero-field (ZF) μSR measurements were performed at the SμS facility at PSI (Switzerland) and the ISIS Muon Facility. In a μSR experiment (for a review of the technique see, for example, Ref. 15), almost 100% polarized positive muons are implanted in the samples where, after a short thermalization ($<10^{-10}$ s), they start precessing about the local magnetic fields. In their decay (with decay constant $\tau = 2.2 \times 10^{-6}$ s) a positron is emitted preferentially in the direction of the muon spin direction at the instant of decay. The time histograms of positron counts, $N_F(t)$ and $N_B(t)$ collected in detectors placed in the forward (F) and backward (B) positions relative to the initial muon polarization thus measure the time evolution of the muon polarization. The muon spin relaxation function (or *asymmetry*) $A(t)$ is given by

$$A(t) = \frac{N_B(t) - \alpha N_F(t)}{N_B(t) + \alpha N_F(t)} = a_0 P_z(t) + a_{bk}, \qquad (1)$$

where a_{bk} is the contribution from muons stopped outside the sample and α is an instrumental parameter that accounts for the forward/backward detector efficiency. $P_z(t)$ describes the muon depolarization inside the specimen and thus provides information on the time evolution of the internal fields. From comparison with what is found in other oxide systems,[16] we assume the muons to be located close to (at about 1 Å) the oxygen atom in the cubic structure over most of the temperature range under study. Hopping might occur at the highest temperatures but, still, the muon spin relaxation will be largely dominated by the fluctuations of the large iron moments.

III. RESULTS

A. Static critical behaviour

Figure 1 shows the temperature dependence of the dc and ac susceptibility for $SrFe_{0.8}Co_{0.2}O_{3.0}$. As expected from previous reports on this system, the dc susceptibility shows a sharp increase at about 250 K signaling the paramagnetic-ferromagnetic (PM-FM) transition. This rise, however, is followed by a strong divergence of the zero-field-cooled (ZFC) and field-cooled (FC) curves, which has been interpreted in similar oxides systems as evidence of the absence for LRO and the presence, instead, of large but finite ferromagnetic clusters.[17] The real part of the ac susceptibility χ' shows no singular behavior at $T_c = 237(1)$ K (obtained from the Kouvel-Fisher analysis, see below), but a maximum (the Hopkinson peak,[18] noncritical) is observed at slightly lower temperature ($\simeq$228 K). Below this point, it decreases monotonically down to 2 K. The ZFC dc data, on the other hand, show a shoulder at about 100 K followed, on cooling, by a rapid decrease in the susceptibility.

The inverse dc susceptibility is displayed in Fig. 2 up to roughly 2 T_c. Its behavior is Curie-Weiss-like at high temperatures but departs from it below ~400 K. Similar behavior has been observed in the cobaltites, in which (as it will be argued for the present case) ferromagnetically ordered clusters form at temperatures significantly higher than T_c.[19] As for those materials, the deviation from the CW prediction

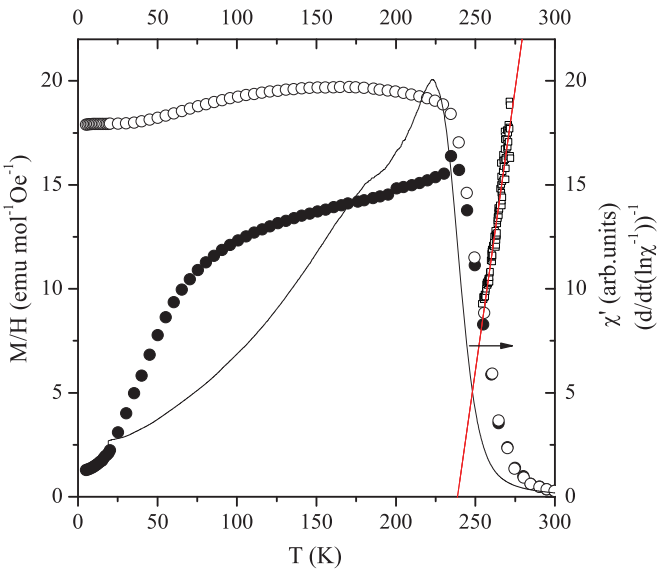

FIG. 1. (Color online) Zero-field-cooled (•) and field-cooled (○) dc-susceptibility data for $SrFe_{0.8}Co_{0.2}O_{3.0}$ in $h_{\text{appl}} = 100$ Oe. Solid line: temperature dependence of the real part of χ_{ac} ($h = 1$ Oe). Open squares: Kouvel-Fisher $(\frac{\partial \ln\chi^{-1}}{\partial T})^{-1}$ vs T plot for determination of γ.

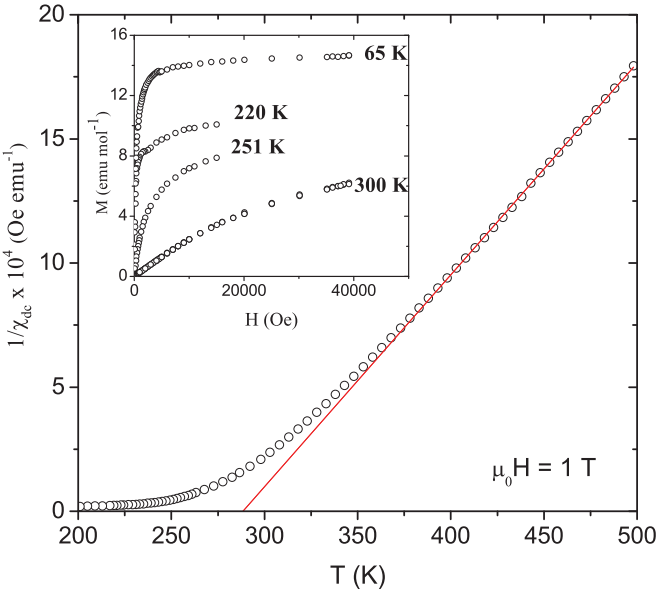

FIG. 2. (Color online) Temperature dependence of the inverse dc susceptibility for an applied field of 1 T showing the departure from Curie-Weiss behavior below ∼400 K. Inset: Characteristic isothermal magnetization curves at various temperatures. The sigmoidal shape of the 300-K data suggests the presence of FM clusters above T_c.

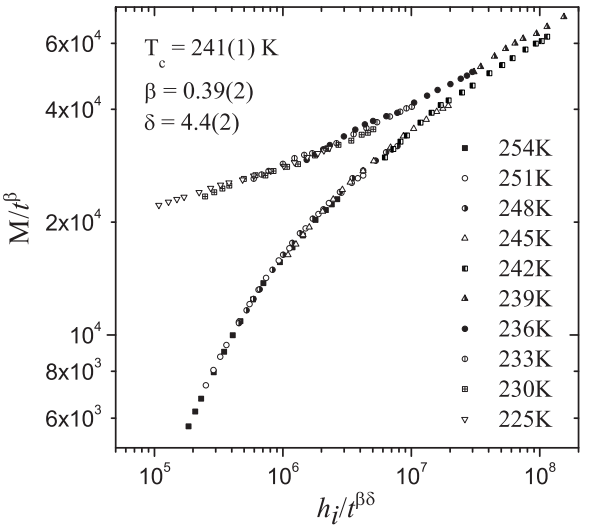

FIG. 3. Scaled magnetization of $SrFe_{0.8}Co_{0.2}O_{3.0}$. The plot shows the collapse of the data onto two curves, one above and one below T_c as expected for a well-defined continuous phase transition.

is upward (i.e., lower susceptibility) thus distinguishing the inhomogeneity in the present case from a true Griffiths phase,[20] for which the deviation in the $1/\chi$ vs T plot should be downward. The ferromagnetic character of these clusters is also hinted from the sigmoidal shape of the isothermal magnetization curve at 300 K plotted in the inset of Fig. 2.

In order to analyze in detail the nature of the ordering transition, isothermal magnetization curves were collected for various temperatures above and below T_c (several characteristic curves are plotted in the inset of Fig. 2). The continuous character of the transition was first confirmed by using the so-called Banerjee criterion,[21] which establishes that, in a h/m vs h^2 Arrott plot, the slope of the linear part of the magnetization isotherms is positive if the transition is continuous and negative if first order. The slope was found to be positive in the present case (not shown).

For a continuous PM-FM phase transition, the various quantities of interest (magnetization, susceptibility, specific heat, etc.) show near the critical point a power-law dependence on the two relevant scaling fields, $t \equiv (T - T_c/T)$ and $h \equiv h_i/k_bT_c$. The transition is thus characterized by a set of exponents defined as follows:

$$M_S(T) = m_0(-t)^\beta, \quad t < 0, h = 0,$$
$$\chi_0^{-1}(T) = (h_0/m_0)t^\gamma, \quad t > 0, h = 0,$$
$$M(T) = Dh^{1/\delta}, \quad t = 0$$

where m_0, (h_0/M_0), and D are the critical amplitudes and β, γ, and δ are the critical exponents for the spontaneous magnetization M_s, initial susceptibility χ_0, and critical magnetization, respectively. A number of equalities relating the different exponents limits to 2 the number of them that are independent.

The conventional analysis of the critical behavior is based on the static scaling hypothesis,[22] according to which the equation of state in the critical regime is given by

$$m(h,t) = |t|^\beta F_\pm(h/|t|^{\beta\delta}), \tag{2}$$

where $F_\pm$ (F_+ for $T > T_c$ and F_- for $T < T_c$) is an unspecified scaling function. The above equation leads to the mentioned power-law dependence of the magnetic parameters. Also, it implies that, for the right choice of critical exponents, M/t^β data near the critical point plotted as a function of $h/t^{\beta\delta}$ should collapse onto two curves, for T above and below T_c, respectively.

Isothermal magnetization curves about the transition are thus presented in Fig. 3 in a log-log plot of the scaled variables M/t^β and $h_i/t^{\beta\delta}$ in the range $-6.2 \times 10^{-2} \leqslant t \leqslant 5.8 \times 10^{-2}$. The plot was obtained by an iteration method starting with three-dimensional (3D) Heisenberg exponents and an initial value of T_c estimated from the ac-susceptibility data using the Kouvel-Fisher method.[23] β and δ were then allowed to vary until the best scaling was obtained. In order to check that the analysis was performed within the asymptotic critical regime (ACR),[24] we carried out the standard procedure of progressively reducing the t range. Had the original fitting included points beyond the ACR, the quality of the scaling would decrease as we reduce the temperature range keeping the exponents fixed since these would in fact be effective average values. We found, however, that no significant distortions of the scaling occurred when the range was reduced to $-8.3 \times 10^{-3} < t < 4.1 \times 10^{-3}$. The derived exponents and T_c are listed in Table I (*scaling I* results).

A second, alternative form of the scaling equation was used in order to determine β and γ independently. Based on the Widom equality, $\gamma = \beta(\delta - 1)$, the equation $m'^2 = \pm a_\pm + b_\pm(h'/m')$ (where $m' \equiv M/t^\beta$ and $h' \equiv h_i/t^{\beta+\gamma}$) implies that the M-H isotherms in the critical regime should fall onto two universal curves in a plot of m'^2 vs h'/m through a proper choice of T_c, β, and γ. This scaling plot yields the values of the critical amplitudes m_0 and h_0/m_0 directly from the intercept of

TABLE I. Derived critical exponents for $SrFe_{0.8}Co_{0.2}O_{3.0}$.

Method	T_c (K)	β	γ	δ
$d\chi/dT$	250(10)			
Kouvel-Fisher	239(1)		1.82	
Scaling I	241(1)	0.39(2)	(1.33)[a]	4.40(2)
Scaling II[b]	241(1)	0.39(1)	1.36(2)	(4.49)
Modified Arrott	∼242	0.41(3)	1.40(15)	(4.41)
3D Heisenberg[c]		0.3689(3)	1.3960(9)	4.783(3)
Mean field		0.50	1.0	3.0

[a]Values in brackets were obtained from the other exponents using the Widom equality.
[b]Best experimental estimates of the critical exponents.
[c]Reference 28.

the two curves with the m'^2 and h'^2/m^2 axes, respectively. The result of the analysis is plotted in Fig. 4. The derived values of the exponents are listed in Table I (as *scaling II*) and those of the amplitudes in Table II. The latter are given as the ratios $m_0/M_s(0)$ and $\mu(0)h_0/k_BT_c$, where $M_s(0)$ and $\mu(0)$ are the 0-K saturation magnetization and saturated magnetic moment, which were estimated from the magnetization isotherm at 5 K.

Further estimates of the values of the β and γ exponents were obtained from yet a third different type of scaling plots, the so-called modified Arrott plots[25] (not shown).

B. Spin dynamics: μSR results

Figure 5(a) shows the thermal evolution of the muon depolarization rate λ(T) derived from the fit of the experimental depolarization curves collected in ISIS in a small longitudinal field of 15 G (which quenches the depolarization due to nuclear dipoles) to a power exponential

$$A(t) = a_0 \exp[-(\lambda t)^s] + b_k, \tag{3}$$

where a_0 is the initial asymmetry at $t = 0$. The exponent s (note that we have avoided the commonly used β in order to avoid confusion with the magnetization critical exponent) measures the spread in relaxation times (see below). As expected

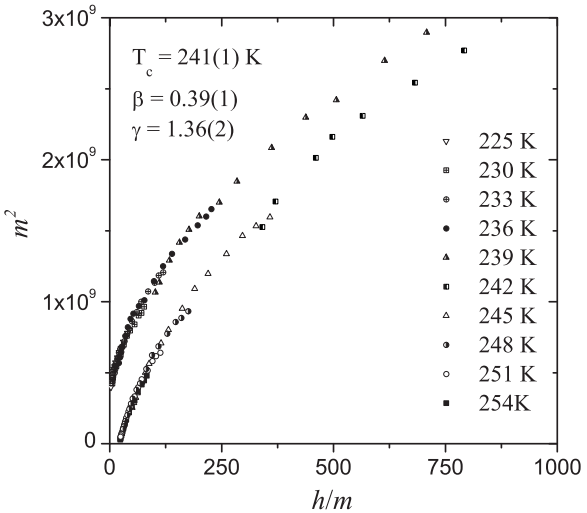

FIG. 4. m'^2 vs h'/m' scaling plot for $SrFe_{0.8}Co_{0.2}O_{3.0}$ ($m' = M/t^\beta$ and $h' = h_i/t^{\beta+\gamma}$).

TABLE II. Experimental values and theoretical predictions of the reduced critical amplitudes.

	$m_0/M_s(0)$	$\mu_0 h_0/k_B T_c$
Experimental	1.38	0.32
3D Heisenberg	1.37	1.58
Mean field	1.73	1.73

from the susceptibility results, $\lambda(T)$ rises as $T \to T_c^+$ signaling the slowing down of spin fluctuations as the transition is approached. Its evolution is, however, somewhat anomalous in that $\lambda(T)$ does not peak at T_c as one would expect for "standard" critical behavior, but at lower temperature. The reason for this apparently "anomalous" behavior can be linked to the values derived for the static critical exponents and will be discussed in the following section.

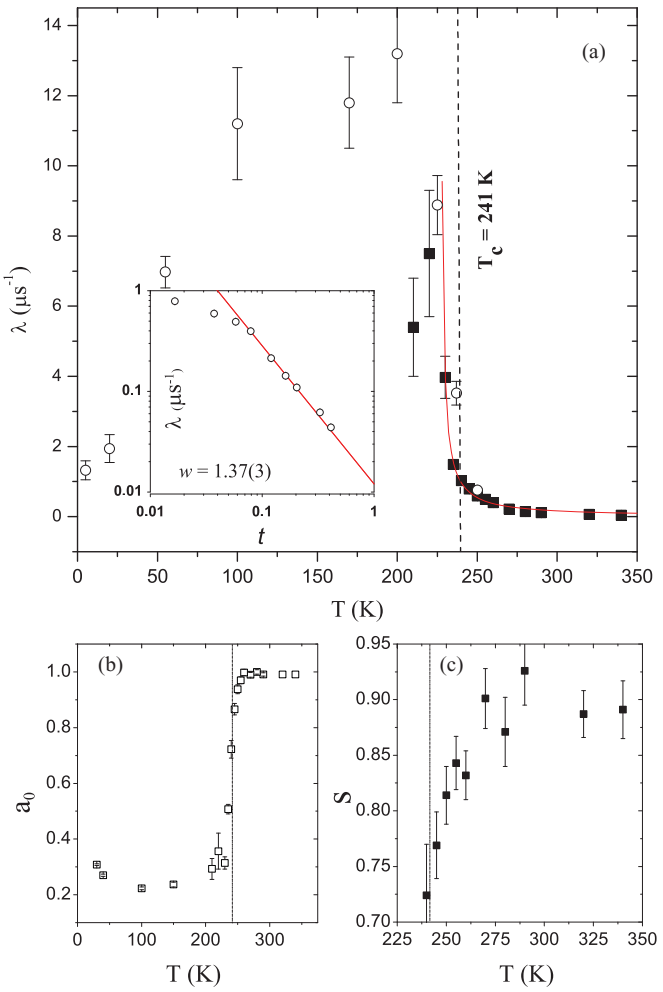

FIG. 5. (Color online) Thermal evolution of the dynamical muon depolarization rate $\lambda(T)$ (a, ■ symbols), initial asymmetry a_0 (b) and β exponent (c) derived from the analysis of the ISIS data. In (a) ○ represent the $\lambda(T)$ derived from the fit of the PSI data to Eq. (4). The solid line represents the fit of the ISIS data above T_c to a power law with the critical temperature as a free parameter. Inset: Fit of the ISIS data to the same power law with fixed $T_c = 241$ K from the scaling analysis above. It yields a dynamical exponent $w = 1.37(3)$.

The evolution with T of a_0 and and s is shown [Figs. 5(b) and 5(c), respectively]. The drop in a_0 observed on cooling through the transition is a consequence of the limited frequency resolution of the ISIS pulsed beam. For a ferromagnetic system in polycrystalline or multidomain form, below T_c, the internal static field is so strong that 2/3 of the initial asymmetry is lost due to the precession about the two transverse components of the field, leaving a value $a_0 = 1/3$, arising from the longitudinal field component. The observed drop in a_0 thus reflects the development of static internal fields (i.e., ferromagnetic ordering) on cooling. What is interesting, however, is that this drop begins at temperatures significantly higher than T_c (at about 270 K). In fact, at T_c, almost 1/3 of the total asymmetry has been already lost. This is consistent with the susceptibility data in Fig. 2 and indicates an inhomogeneous nature of the paramagnetic regime above T_c with slowly fluctuating or even static ferromagnetically ordered regions (clusters), responsible for the decrease in a_0, coexisting with a rapidly fluctuating nonordered matrix. The relative weight of each component changes with temperature. The thermal dependence of s also shows evidence of this inhomogeneity. In the fast fluctuating regime, $\lambda \propto \gamma_v^2 \Delta^2 \tau_c$ (where Δ is the width of the internal field distribution sensed by the muon, $\gamma_v = 135.5\ \mathrm{MHzT}^{-1}$ is the muon gyromagnetic ratio and τ_c is the average spin-spin correlation time). That is, $\lambda(T)$ reflects the T evolution of the average correlation time. Thus for a system of uncorrelated, rapidly fluctuating spins characterized by a single τ_c, the depolarization is single exponential, i.e., $s = 1$. Deviation from this behavior $\lambda(T)$ ($s < 1$) is usually taken as evidence of a (broad) distribution of correlation times. In the present case, the spread in τ_c and subsequent drop in s (starting at temperature well above T_c) is consistent with the development of an inhomogeneous distribution of internal fields due to the phase separation mentioned above. In other words, the drop in β reflects the formation of the ferromagnetic clusters already in the paramagnetic regime and the evolution into a inhomogeneous ordered state below the transition (characterized by $s = 0.5$).

In order to study the nature of the ordered phase below T_c, data were collected at PSI, a continuous source. A preliminary analysis of these data was published elsewhere.[26] In this case, the increased resolution allowed us to resolve the high-frequency precession signals anticipated for the case of long-range magnetic ordering (Fig. 6). The characteristic oscillations of an ordered magnet are, however, heavily damped for this material and essentially gone for $t > 0.1\ \mu$s, indicating, again, a large spread in internal fields at the muon site and therefore an inhomogeneous ground state also below T_c. The situation is analogous to that reported for $La_{0.67}Ca_{0.33}MnO_3$.[27] As for that system, the data are well described by a function

$$A(t) = a_1 \exp(-\sigma t)\cos(\omega_\mu t + \phi) + a_2 \exp[-(\lambda t)^s] + b_k, \tag{4}$$

where the first term, missing in the ISIS data, accounts for the damped oscillations arising from the transverse field components (σ is the inhomogeneous linewidth arising from the spread of internal fields and ω_μ is the muon precessing frequency) and the second for the spin-lattice relaxation of the longitudinal component, as before. Figure 7 shows the temperature dependence of the derived precessing frequency ω_μ. The quasilinear increase on cooling is unusual and distinct from the expected behavior for a well-behaved ferromagnet (i.e., $\omega_\mu \propto t^\beta$; with β the magnetization critical exponent). We do not have an explanation for this behavior at the moment but it is probably related to the glassy dynamics observed for the system.

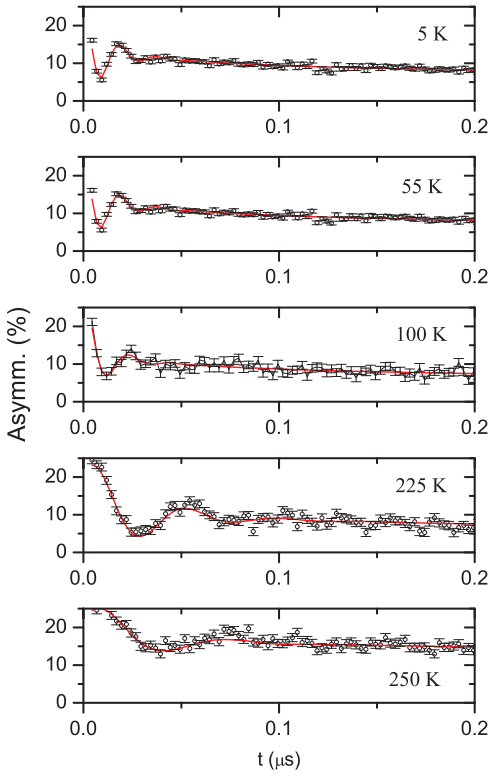

FIG. 6. (Color online) PSI time-dependent asymmetry for $SrFe_{0.8}Co_{0.2}O_{3.0}$ at several temperatures. The solid lines are the best fits of the experimental data to Eq. (4).

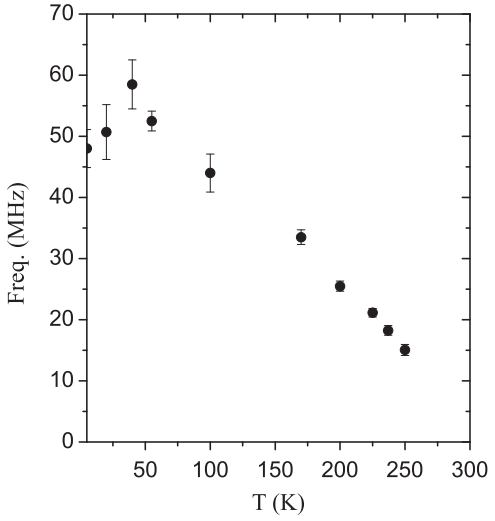

FIG. 7. muon spin precession frequency for $SrFe_{0.8}Co_{0.2}O_{3.0}$ derived from the fit of the PSI data to a damped oscillation added to a exponentially relaxing component [Eq. (4)].

Finally, it is worth noting that a resolvable oscillating component (accounting for a smaller fraction of the total asymmetry than at temperatures below T_c where it is the majority one) is observed in the depolarization curve at 250 K, above the ordering temperature, further confirming the picture that emerges from the analysis of the ISIS data above of ferromagnetically ordered regions (clusters) segregated from the paramagnetic background at $T > T_c$.

IV. DISCUSSION

A. Effect of disorder on the transition

The above analysis confirms the onset of long-range ferromagnetism below a well-defined continuous PM-FM transition at ∼241 K since it is only in this case that the scaling hypothesis is satisfied and the magnetic isotherms collapse, as in Figs. 2 and 3, and the critical exponents comply to the constrains imposed by the different scaling relations (note that Figs. 2 and 3 are only equivalent because of the Widom equality). The derived exponents, listed in Table I, are close to those of the 3D Heisenberg model with short-range exchange interactions,[28] as predicted for double-exchange systems[29] and thus in line with what is experimentally observed in many double-exchange manganites (Ref. 30, and references therein) and cobaltites (Ref. 31).

However, the first thing one notices in Table I is the large discrepancy that exists between the values of γ calculated using the KF (1.82) and scaling analysis (1.36). This can be interpreted as arising from the presence of disorder. As indicated, without adding further "correction-to-scaling" terms to the expressions above, the true critical exponents can only be obtained from data within the asymptotic critical regime. Outside of this the analysis yields average effective values that differ from the predictions for the different universalities. In the case of γ, in the ACR, both ordered and disordered ferromagnets behave alike, but for $t > t_0$ (t_0 being the reduced crossover temperature that marks the end of the ACR) their behavior diverges: Whereas ordered magnets show a monotonic decrease from the temperature-independent ACR value toward the mean-field value of 1 as the system is heated into the paramagnetic regime, for disordered magnets, the effective γ goes first through a maximum (larger than the ACR value) at $t_{\max} = 0.1$–0.5 and finally decreases to 1.[32,33] In order to check that this is indeed what happens for $SrFe_{0.8}Co_{0.2}O_{3.0}$, we have analyzed the power dependence of the linear ac susceptibility [$\chi^{-1} = (h_0/M_0)t^{\gamma}$] for different t ranges. If the fitting range is reduced to the one used in the scaling analysis above ($t < 0.06$), the value obtained is $\gamma = 1.39$, in good agreement with the result of scaling. If, on the other hand, the range is extended to that used in the KF analysis ($0.055 < t < 0.12$) the resulting exponent ($\gamma = 1.82$) is similar to the one obtained with that method.

Clearly, the use of a wider t fitting range beyond the ACR yields a higher effective exponent, which, as indicated, constitutes further confirmation of a disordered magnetic state presence. The origin of this disorder can be tentatively explained by considering the evolution of the magnetic ground state with x along the $SrFe_{1-x}Co_xO_{3.0}$ family. Circular dichroism studies by Okamoto and co-workers[34] have confirmed what was already suggested by previous magnetization studies, especially that of Kawasaki;[5] that is, that the ferromagnetic polarization of the Fe magnetic moments increases with doping, induced by the interaction with the doped Co moments. This destroys the antiferromagnetic helical structure in the first place and then gives rise to a spin-glass and re-entrant spin-glass behavior for $x = 0.10$ and 0.15, respectively.[35] In the latter, the magnetism can be tentatively explained in terms of the presence of large ferromagnetic clusters in a glassy matrix. For $x = 0.20$, the results above show that FM LRO exits bellow a well-defined continuous transition T_c, meaning that at T_c, the spin-correlation length diverges. However, this does not preclude the existence of nonpercolating clusters of different magnetic nature embedded within the percolating ferromagnetic matrix. In fact, the susceptibility and μSR data above are indicative of the "preformation" of ferromagnetically ordered clusters at temperatures above the onset of true LRO.[1,19] As T_c is approached, these clusters grow in size and percolation occurs for some of them, not all. The result is that only a fraction of the total number of spins participate in the transition. Evidence of this can be extracted from the comparison of the derived value of $\mu(0)h_0/k_BT_c$ with the prediction for a 3D Heisenberg system (Table II). The experimental value is significantly smaller than the predicted one. If h_0 is taken to be an effective exchange field and μ_0 is the average effective moment involved in the PM-FM transition, at T_c, the effective exchange energy $\mu_{\text{eff}}h_0$ is expected to equal the thermal energy k_bT_c, which is not the case in the present case unless μ_{eff} adopts a value of $8.5\mu_B$, much higher than $\mu(0) = 2.69\mu_B$ required for the ratio $\mu(0)h_0/k_BT_c$ to take the Heisenberg value of 1.58. As argued by Kaul,[36] the reason for this discrepancy is that, as suggested above, only a fraction $c = \mu_{\text{eff}}/\mu(0)$ of the spins takes part in the transition, $c = 32\%$ for $SrFe_{0.8}Co_{0.2}O_{3.0}$.

Finally, it is important to notice that, despite the inhomogeneous nature of the magnetic system and the fact that only a portion of the spins form the matrix that percolates at T_c, the derived critical exponents listed in Table I still provide an accurate description of the transition. According to the so-called Harris criterion, quenched disorder is irrelevant in the ACR in systems for which α, the specific-heat critical exponent, is negative.[37,38] In the absence of a direct measurement, we can estimate α from the values of the other exponents via the scaling equality $\alpha = 2(1 - \beta) - \gamma$, which results in $\alpha = -0.14$ for the present system. Hence having established that the values listed in Table I (scaling I) are true ACR exponents, they are unaffected by the disorder and thus are the same we would obtain for the corresponding homogeneous system.

B. Heisenberg to mean-field drift due to long-range dipolar interactions

As noted above, the derived values are essentially those of a 3D system of Heisenberg spins. However, a closer look reveals a slight but definitive deviation toward the mean-field predictions in the three exponents. The size of the deviation makes it arguable whether it represents a true drift or simply a random oscillation about the Heisenberg values. However, the fact that the change occurs in the right direction for the

three exponents leads us to believe that the deviation is not random but represents a definite tendency toward mean-field behavior. In this sense, it is worth comparing the current values with those reported by Seeger for Ni [$\beta = 0.395(10)$, $\gamma = 1.345(10)$, and $\delta = 4.35(6)$], with a well-established drift from 3D Heisenberg (3DH) behavior toward mean field due to long-range interactions involving the itinerant electrons.[32] In a homogeneous magnet, for a given symmetry, the universality class of the transition is determined by the range of the interactions J(r). A renormalization-group study by Fisher and co-workers showed that $J(r) = 1/r^{d+\sigma}$ where d is the dimensionality of the system and σ is a measure of the range of the exchange interaction.[39] A 3D system of isotropic spins complies with the Heisenberg model only if $\sigma > 2.0$, i.e., if $J(r)$ decreases with distance faster than r^{-5}. Mean-field exponents are obtained for $J(r) \propto r^{-n}$ with $n \leqslant 4.5$. In the intermediate range, i.e., for $J(r) \propto r^{-3-\sigma}$ with $3/2 \leqslant \sigma \leqslant 2.0$, the system belongs to a different class with exponents that take intermediate values depending on σ. σ must be close to 2 in the present system ($\sigma = 1.91$ for Ni, with a similar magnitude for the deviation from 3DH behavior[32]).

In principle, the intermediate range of the interactions, and thus the deviation from pure 3DH character, in $SrFe_{0.8}Co_{0.2}O_{3.0}$ could be ascribed to the long-range nature of the double-exchange coupling. However, Monte Carlo simulations by Motome and Furukawa[29] suggest that the long-range part of the magnetic interactions in the double-exchange models are renormalized to the point of being irrelevant and so the systems should behave as short ranged. The result is supported by the large number of manganite compositions that are found experimentally to display 3DH character.[30]

Alternatively, the crossover toward mean-field exponents could result from the presence of isotropic long-range dipolar interactions (IDL). Renormalization-group calculations show that isotropic 3DH criticality is unstable against IDL perturbations and a crossover from 3DH to IDL critical behavior occurs at a certain value t_{co} of the reduced temperature that depends on the strength of the dipolar interactions.[32,40] According to these calculations, the values of the new exponents characterizing the IDL regime are only slightly different from the corresponding Heisenberg values and shifted toward mean field. The theory also predicts that the effective γ^* exponent should go through a minimum as a result of the crossover. This appears to be in contradiction to our results, which show that γ^* increases as we move away from T_c due to the presence of disorder. In fact, the reason for this apparent disagreement is the temperature range in which the exponent is calculated, as it is only for $t < t_{co}$ that the system is governed by dipolar interactions and the new regime sets in. t_{co} can be estimated as $t_{co} \approx g_d^{1/\phi_d}$, where g_d is a measure of the dipolar interactions and ϕ_d is the crossover exponent.[41] $\phi_d \approx \gamma_H = 1.39$,[32,41] whereas g_d can be calculated[40,41], as $g_d \approx \frac{0.87}{T_c}\frac{\theta \cdot p^2}{V}$, where θ is a constant that depends on S, the total spin number and which, following Ref. 41, we take to be 0.80 for $S \sim 2$ in the current system; $p = 4.899\mu_B$ (for $S = 2$) is the calculated magnetic moment and $V = 56.76$ Å^3 is the unit-cell volume. This results in $g_d \approx 1.2 \times 10^{-4}$ and $t_{co} \approx 1.3 \times 10^{-3}$. $\gamma^* = 1.89$ was calculated in a range $0.055 \leqslant t \leqslant 0.12$, i.e., away from the IDL regime and thus shows the expected behavior of a short-range system in the presence of disorder. The t range used in the calculation of the exponents by the different scaling methods ($t \geqslant 3 \times 10^{-3}$) is, on the other hand, close to the estimated crossover to IDL behavior and so their values reflect the effect of the new regime.

This crossover from a short-range Hesisenberg critical behavior to a dipolar-dominated regime characterized by a slight drift toward mean-field exponents can be further corroborated by the analysis of the critical spin dynamics obtained from the μSR data. As indicated, $\lambda \propto \gamma_\nu^2 \Delta^2 \tau_c$. The increase in $\lambda(T)$ observed on cooling thus results from the critical slowing down of spin fluctuations as $T \rightarrow T_c^+$, that is, from the divergence of the correlation time as the transition is approached. In that case, $\lambda(T)$ can be described by a power law $\lambda(T) = \lambda_0 t^{-w}$, where w is the critical exponent for the correlation time according to the theory of dynamic critical phenomena.[42] However, Fig. 4 shows that, for $SrFe_{0.8}Co_{0.2}O_{3.0}$, $\lambda(T)$ continues to rise below the transition and only peaks at T well below T_c, i.e., it appears as if τ_c was nondivergent at T_c. A similar behavior was observed in $Nd_{0.5}Sr_{0.5}MnO_3$ by Krishnamurthy *et al.*,[43] who also evoked the role of long-range dipolar interactions to explain it. Dipolar interactions induce q anisotropy in the otherwise isotropic susceptibility suppressing the divergence at T_c of the susceptibility due to longitudinal fluctuations while leaving the transverse one virtually unaffected.[40,43,44] The result is that the average correlation time does indeed become nondivergent at T_c. The rise in $\lambda(T)$ is thus less steep than expected for a pure isotropic exchange critical behavior. The exponent w was thus estimated from a log-log plot of the depolarization rate vs reduced temperature but keeping T_c fixed to the value determined from the static scaling analysis above (241 K) (inset of Fig 5). The obtained value, $w = 1.37(3)$ is slightly higher than the theoretical prediction for 3DH ferromagnet (1.023),[43] and agrees well with that reported for Gd [1.39(3)],[45] with a well-established Heisenberg-to-dipolar crossover.[46] Following Suter's approach,[47] we have further checked the validity of this interpretation calculating the effective generalized dynamical exponent z from the derived value of w. w is related to other critical exponents by the expression[48]

$$w = \nu(z + 2 - d - \eta), \tag{5}$$

where ν and η are the exponents that describe the divergence of the correlation length and the spin-spin correlation function, respectively,[22] and $d = 3$ is the system dimensionality. $\eta = 0.034$ for a three-dimensional ferromagnet.[48] Without direct measurements of $\xi(T)$, ν can be eliminated from the equation via the scaling relation $z = 2 + \alpha/\nu$ and α can been obtained from the other static exponents ($\alpha = 2 - 2\beta - \gamma = -0.14$). This yields a value of $z \approx 1.91$, which compares well with the prediction for a dipolar ferromagnet (1.98),[42] and the values reported for $Nd_{0.5}Sr_{0.5}MnO_3$ [2.00(12)] (Ref. 43) and Gd [1.8(1)],[45] with similar crossover behaviors. In contrast, it lies significantly lower than the Heisenberg prediction ($z = 5/2$).[48] It is worth noting here that the value of the z exponent reflects that it is dipolar interactions and not electron delocalization that produces the observed deviation from Heisenberg critical behavior. *A priori*, both could act as the perturbation to short-range exchange interactions that causes the crossover.

However, it has been shown that for delocalized electrons, z remains equal to $5/2$ for all values of t,[49] thus excluding this mechanism as the origin of the observed behavior.

V. CONCLUSIONS

The analysis of the critical behavior in $SrFe_{0.8}Co_{0.2}O_{3.0}$ shows that, like most double-exchange manganites and cobaltites away from multicritical points, it behaves as expected for a system of Heisenberg spins coupled by short-range interactions. The dipolar interactions between the Fe(IV) centers introduce, however, a perturbation to this picture and dominate the critical behavior as $t \to 0$ producing a slight change of the critical exponents away from the Heisenberg predictions.

Our study of the transition shows as well that the system is magnetically inhomogeneous at all temperatures. Ferromagnetically ordered clusters separate from the paramagnetic background at a temperature well above T_c in a situation analogous to that found in manganites and cobaltites. The size of these clusters increases as $T \to T_c^+$ and, at the transition, percolation occurs for some of them. Only a fraction of the spins participate in the infinite percolating cluster. The μSR data below the transition are also interpreted in terms of spatial inhomogeneity of the spin-spin correlations times.

ACKNOWLEDGMENTS

The authors wish to thank the technical staff at both ISIS and PSI for their support during the μSR measurements. Technical support provided by SGIker (UPV/EHU, MICINN, GV/EJ, ESF) is also gratefully acknowledged. Part of this work was financially supported by the Spanish Ministerio de Educación (Project No. MAT2007-66737-C02-01).

*jorge.lago@ehu.es

[1] E. Dagotto, *Nanoscale Phase Separation and Colossal Magnetoresistance* (Springer, Berlin, 2003).

[2] J. Wu, J. W. Lynn, C. J. Glinka, J. Burley, H. Zheng, J. F. Mitchell, and C. Leighton, Phys. Rev. Lett. **94**, 037201 (2005).

[3] Y. Takeda, K. Kanno, T. Takada, O. Yamamoto, M. Takano, N. Nakayama, and Y. Bando, J. Solid State Chem. **63**, 237 (1986).

[4] P. D. Battle, M. A. Green, J. Lago, M. J. Rosseinsky, L. E. Spring, J. Singleton, and J. F. Vente, Chem. Commun. **9**, 987 (1998).

[5] S. Kawasaki, M. Takano, and Y. Takeda, J. Solid State Chem. **121**, 174 (1996).

[6] T. Takeda, Y. Yamaguchi, and H. Watanabe, J. Phys. Soc. Jpn. **33**, 967 (1972).

[7] J. Zaanen, G. A. Sawatzky, and J. W. Allen, Phys. Rev. Lett. **55**, 418 (1985).

[8] A. E. Bocquet, A. Fujimori, T. Mizokawa, T. Saitoh, H. Namatame, S. Suga, N. Kimizuka, Y. Takeda, and M. Takano, Phys. Rev. B **45**, 1561 (1992).

[9] The oxygen hole couples the metal ions antiferromagnetically. In order to do so, the spins of the metal e_g electrons need to be parallel. The large intra-atomic Hund coupling makes then the t_{2g} spins lie parallel to each other.

[10] M. Mostovoy, Phys. Rev. Lett. **94**, 137205 (2005).

[11] R. H. Potze, G. A. Sawatzky, and M. Abbate, Phys. Rev. B **51**, 11501 (1995); P. Bezdicka, A. Wattiaux, J. C. Grenier, M. Pouchard, and P. Hagenmuller, Z. Anorg. Allg. Chem. **619**, 7 (1993).

[12] M. Abbate, G. Zampieri, J. Okamoto, A. Fujimori, S. Kawasaki, and M. Takano, Phys. Rev. B **65**, 165120 (2002).

[13] Note that despite the helicoidal antiferromagnetic spin structure, the dominating interactions in $SrFeO_{3.0}$ are indeed ferromagnetic as indicated by the positive value of the Weiss temperature, $\theta =$ 49 K.

[14] T. Takeda, T. Watanabe, S. Komura, and S. Fujii, J. Phys. Soc. Jpn. **56**, 731 (1987).

[15] S. J. Blundell, Contemp. Phys. **40**, 175 (1999); P. Dalmas de Reotier and A. Yaouanc, J. Phys.: Condens. Matter **9**, 43 (1997).

[16] A. Schenck and F. N. Gygax, *Handbook of Magnetic Materials*, edited by K. H. J. Buschow (North-Holland, Amsterdam, 1995), Vol. 9.

[17] S. Mukherjee, R. Ranganathan, P. S. Anilkumar, and P. A. Joy, Phys. Rev. B **54**, 9267 (1996); M. Itoh, I. Natori, S. Kubota, and K. Motoya, J. Phys. Soc. Jpn. **63**, 1486 (1994); D. N. H. Nam, K. Jonason, P. Nordblad, N. V. Khiem, and N. X. Phuc, Phys. Rev. B **59**, 4189 (1999).

[18] J. Hopkinson, Proc. R. Soc. London **48**, 1 (1890).

[19] C. He, M. A. Torija, J. Wu, J. W. Lynn, H. Zheng, J. F. Mitchell, and C. Leighton, Phys. Rev. B **76**, 014401 (2007).

[20] R. B. Griffiths, Phys. Rev. Lett. **23**, 17 (1969).

[21] B. K. Banerjee, Phys. Lett. **12**, 16 (1964).

[22] H. Eugene Stanley, *Introduction to Phase Transitions and Critical Phenomena* (Oxford University Press, New York, 1971).

[23] According to the Kouvel-Fisher analysis, in the critical regime, the linear susceptibility varies as $\gamma(T) = (T - T_c) \cdot \frac{\partial ln\chi^{-1}}{\partial T} = (T - T_c) \cdot \chi \cdot \frac{\partial \chi^{-1}}{\partial T}$. Thus T_c can be obtained from the intercept on the T axis of a $(\frac{\partial ln\chi^{-1}}{\partial T})^{-1}$ vs T plot. The slope of the linear regression fit of the data yields the effective γ exponent.

[24] It is only in the ACR that the derived exponents truly characterize the critical behavior and are not temperature-dependent averages as would be the case if the temperature range used extended beyond the ACR limit t_0 (of the order of 10^{-2} for ordered magnets and somewhat larger for disordered and amorphous systems (Ref. 32).

[25] A. Arrott and J. E. Noakes, Phys. Rev. Lett. **19**, 786 (1967).

[26] I. M. Marshall, S. J. Blundell, A. Husmann, T. Jestädt, B. W. Lovett, F. L. Pratt, J. Lago, P. D. Battle, and M. J. Rosseinsky, Physica B **289**, 89 (2000).

[27] R. H. Heffner, L. P. Le, M. F. Hundley, J. J. Neumeier, G. M. Luke, K. Kojima, B. Nachumi, Y. J. Uemura, D. E. MacLaughlin, and S. W. Cheong, Phys. Rev. Lett. **77**, 1869 (1996).

[28] M. Campostrini, M. Hasenbusch, A. Pelissetto, P. Rossi, and E. Vicari, Phys. Rev. B **65**, 144520 (2002).

[29] Y. Motome and N. Furukawa, J. Phys. Soc. Jpn. **70**, 1487 (2001).

[30] J. Fan, L. Ling, B. Hong, L. Zhang, L. Pi, and Y. Zhang, Phys. Rev. B **81**, 144426 (2010).

[31] J. Mira, J. Rivas, M. Vázquez, J. M. García-Beneytez, J. Arcas, R. D. Sánchez, and M. A. Señarís-Rodríquez, Phys. Rev. B **59**, 123 (1999); S. Mukherjee, P. Raychaudhuri, and A. K. Nigam,

ibid. **61**, 8651 (2000); N. Khan, A. Midya, K. Mydeen, P. Mandal, A. Loidl, and D. Prabhakaran, *ibid*. **82**, 064422 (2010).
[32]M. Seeger, S. N. Kaul, H. Kronmüller, and R. Reisser, Phys. Rev. B **51**, 12585 (1995).
[33]S. N. Kaul, Phys. Rev. B **38**, 9178 (1988); P. D. Babu and S. N. Kaul, J. Phys.: Condens. Matter **9**, 7189 (1997).
[34]J. Okamoto, K. Mamiya, S. -I. Fujimori, T. Okane, Y. Saitoh, Y. Muramatsu, K. Yoshii, A. Fujimori, A. Tanaka, M. Abbate, T. Koide, S. Ishiwata, S. Kawasaki, and M. Takano, Phys. Rev. B **71**, 104401 (2005).
[35]J. Lago, Ph.D. thesis, University of Oxford, Oxford, 2000.
[36]S. N. Kaul, J. Magn. Magn. Mater. **53**, 5 (1985).
[37]A. B. Harris, J. Phys. C **7**, 1671 (1974).
[38]A. Weinrib and B. I. Halperin, Phys. Rev. B **27**, 413 (1983).
[39]M. E. Fisher, S.-k. Ma, and B. G. Nickel, Phys. Rev. Lett. **29**, 917 (1972).
[40]A. Aharony and M. E. Fisher, Phys. Rev. B **8**, 3323 (1973); M. E. Fisher and A. Aharony, Phys. Rev. Lett. **30**, 559 (1973).
[41]K. Ried, D. Köhler, and H. Kronmuller, J. Magn. Magn. Mater. **116**, 259 (1992).
[42]P. C. Hohenberg and B. I. Halperin, Rev. Mod. Phys. **49**, 435479 (1977).
[43]V. V. Krishnamurthy, I. Watanabe, K. Nagamine, H. Kuwahara, and Y. Tokura, Phys. Rev. B **61**, 4060 (2000).
[44]J. Kötzler, Phys. Rev. Lett. **51**, 833 (1983).
[45]S. Srinath, S. N. Kaul, and H. Kronmüller, Phys. Rev. B **59**, 1145 (1999).
[46]E. Frey, F. Schwabl, S. Henneberger, O. Hartmann, R. Wäppling, A. Kratzer, and G. M. Kalvius, Phys. Rev. Lett. **79**, 5142 (1997).
[47]R. M. Suter and C. Hohenemser, Phys. Rev. Lett. **41**, 705 (1978); L. Chow, C. Hohenemser, and R. M. Suter, *ibid*. **45**, 908 (1980).
[48]G. S. Collins, A. R. Chowdhury, and C. Hohenemser, Phys. Rev. B **33**, 4747 (1986).
[49]J. A. Hertz, J. Magn. Magn. Mater. **1**, 253 (1971); **1**, 303 (1971); C. Hohenemser, L. Chow, and R. M. Suter, Phys. Rev. B **26**, 5056 (1982).